

Sanjay Tikale¹ and K. Narayan Prabhu²

The Effect of Multi-Walled Carbon Nanotubes Reinforcement and Multiple Reflow Cycles on Shear Strength of SAC305 Lead-Free Solder Alloy

Reference

S. Tikale and K. Narayan Prabhu, "The Effect of Multi-Walled Carbon Nanotubes Reinforcement and Multiple Reflow Cycles on Shear Strength of SAC305 Lead-Free Solder Alloy," *Materials Performance and Characterization* 8, no. 3 (2019): 421–433. <https://doi.org/10.1520/MPC20180044>

ABSTRACT

In this study, the effect of multi-walled carbon nanotubes (MWCNT) reinforcement on joint shear strength and microstructural development of tin-3.0silver-0.5copper (SAC305)/copper solder joint subjected to multiple reflow cycles was investigated. The MWCNT-reinforced SAC305 solder systems (SAC305-x MWCNT; $x = 0.01, 0.05, 0.1, \text{ and } 0.5 \text{ wt.}\%$) were developed by a mechanical dispersion method. The microstructural, mechanical, and melting properties of SAC305 composite solders were evaluated as a function of different wt.% of MWCNT addition. The melting behavior of composite solders was analyzed using differential scanning calorimetry. The morphology and intermetallic compound growth at the solder joint interface were studied using scanning electron microscopy. The copper/solder/copper micro-lap-shear solder joint specimens reflowed for multiple reflow cycles were systematically characterized to evaluate the joint shear strength. The results showed that the reinforcement in the range of 0.01–0.05 wt.% of MWCNT resulted in the improvement of joint shear strength and better wettability compared to plain SAC305 solder alloy. Amongst all compositions analyzed, SAC305-0.05MWCNT nanocomposite suppressed the intermetallic compound layer growth effectively leading to improvement in the joint shear strength under multiple reflow cycles.

Keywords

lead-free solder, multi-walled carbon nanotubes, nanocomposite, multiple reflow cycles, shear strength

Manuscript received March 6, 2018; accepted for publication May 29, 2018; published online May 10, 2019.

¹ Department of Metallurgical and Materials Engineering, National Institute of Technology Karnataka, Surathkal, Mangalore 575025, India

² Department of Metallurgical and Materials Engineering, National Institute of Technology Karnataka, Surathkal, Mangalore 575025, India (Corresponding author), e-mail: prabhukn_2002@yahoo.co.in, <https://orcid.org/0000-0002-8359-2587>

Introduction

Tin-silver-copper (Sn-Ag-Cu [SAC]) lead-free solders are now widely used in electronic packaging industries because of their excellent mechanical properties, good solderability, and low environmental damages. SAC solder alloy compositions have proved their dominance among the tin-based solders as the best substitute options for tin-lead solders because of their performance and effectiveness.¹ Solder alloys used in densely packed electronic devices must possess the essential properties to withstand the mechanical loads and adverse effects associated with the high homologous temperature developed throughout the service life of such devices. In recent times, research has shown that the addition of alloying elements often improves the properties of lead-free solders.^{2,3} Development of nanocomposite solders has been successfully proved as a potential and viable way to enhance the solder strength and reliability of the conventional lead-free solders.⁴ One such prominent material that grabs a considerable amount of attention from researchers is carbon nanotubes (CNT). Studies showed that CNT exhibit exceptional physical, thermal, electrical, and mechanical properties.⁵ Because of their unique properties, reinforcement of CNT in lead-free solder alloys is considered to be a promising option in the development of composite solders.⁶

Study on SAC-CNT composite solder done by Nai, Wei, and Gupta⁷ showed that the CNT composite solder has better wettability and dimensional stability over plain SAC solder. The composite solder possesses a lower coefficient of thermal expansion, improved tensile strength, and creep resistance. Investigation on the addition of single-wall carbon nanotubes (SWCNT) in SAC solders showed the reduction in the size of the secondary phases of the composite solder. The composite solder exhibited enhanced hardness and ultimate tensile strength with an increase in SWCNT wt.% addition but at the cost of the reduction in the solder joint ductility.⁴ Another study by Nai et al.⁸ suggests that the addition of CNT in various amounts improves the microhardness and overall strength of the solder matrix and has minimal influence on intermetallic compounds (IMC) growth during soldering. Xu et al.⁹ studied the effect of CNT addition on electroless nickel-phosphorous under bump metallization for lead-free solder interconnections. The result showed the enhancement in bond strength because of CNT addition under multiple reflows. Investigation on the addition of multi-walled carbon nanotubes (MWCNT) in tin-5 antimony (Sn-5Sb) lead-free solder showed the slight decline in melting temperature of the composite solder alloy. The study also indicates the retardation of IMC growth at tin-5 antimony/copper joint interface under thermal aging.¹⁰ The effect of CNT addition on the intermetallic formation and shear strength of tin-3.5 silver (Sn-3.5Ag) solder alloy was investigated by Mayapan et al.¹¹ and the study showed the retardation of Cu_6Sn_5 and Cu_3Sn IMC growth rate and improvement in the joint shear strength with nanoparticles addition. Researchers have made efforts to improve the thermal and electrical properties along with mechanical properties of lead-free solder alloys with CNT addition to make composite lead-free solders more suitable in electronic applications. Lee et al.¹² have reported the improvement in thermal conductivity of tin-MWCNT-reinforced tin-58 bismuth (Sn-58Bi) composite solder alloy. Studies by Kim et al.¹³ showed the improvement in electrical conductivity and thermo-mechanical properties for MWCNT/indium-tin-bismuth (In-Sn-Bi) composite solder alloy reflowed on polyethylene terephthalate substrate. In recent studies, Yang, Liu, and Zhang¹⁴ investigated the tensile-creep behavior of CNT-reinforced tin-58 bismuth solder alloy. The result showed that the addition of CNT refined the solder microstructure and suppressed the IMC thickness at the joint interface. The study also highlights that the improvement in tensile creep resistance of composite solder is superior to plain solder alloy. Sun, Chan, and Wu¹⁵ investigated the effects of CNT and nickel-coated CNT on the reliability of tin 57.6 bismuth-0.4 silver (Sn-57.6Bi-0.4Ag) solder alloy. The findings suggest that the solder doped with less than 0.05 wt.% CNT showed the better dispersion of CNT in the molten solder and largely improved the mechanical performance of the solder joint.

Electronic interconnects often go through multiple reflow cycles during manufacturing and repair activities. The intermetallic compound layers at the solder/substrate interface generally grow thicker with repeated exposure to the high-temperature environment. The IMC is particularly brittle in nature. A thin and uniform IMC layer at the interface enhanced the solder joint bonding and provided mechanical strength

FIG. 1 (A) SEM image of MWCNT, (B) TEM image of MWCNT, (C) TEM image showing inner and outer diameter range of multi-walled carbon nanotube, and (D) XRD pattern for MWCNT.

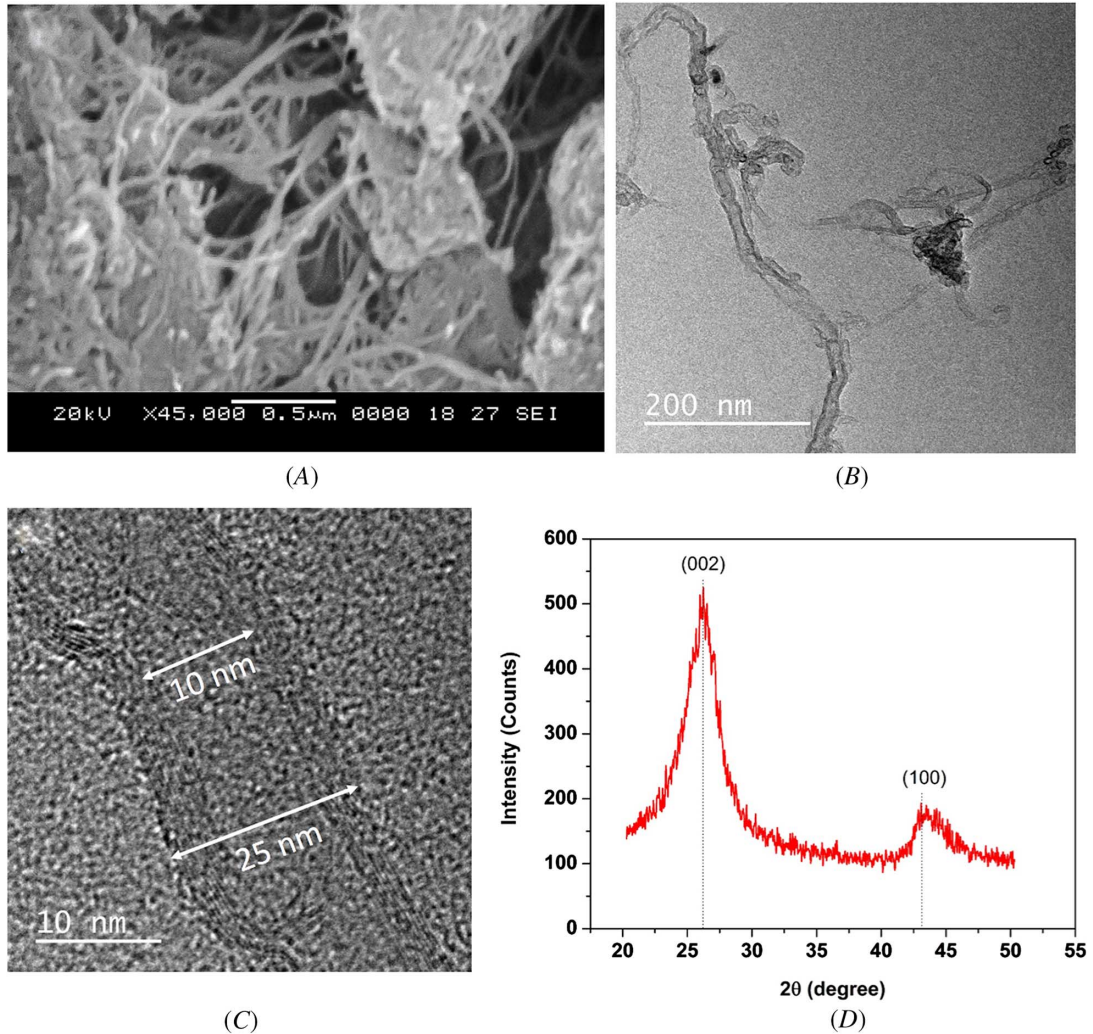


FIG. 2 Schematic diagram of micro-lap-shear solder joint.



to the joint. However, thick IMC layer at the interface often possesses microcracks that decrease the solder joint strength under stress. The motivation for the development of nanocomposite solder alloy with MWCNT addition is to improve the solder properties and suppress the IMC growth when the solder joint is exposed

to multiple reflow cycles, thereby improving the solder performance. The effect of carbon nanotubes reinforcement on mechanical properties and interfacial IMC growth of the solder joint under repeated reflow cycles is largely unexplored. The objective of this study is to investigate the effect of the addition of MWCNT on the solder joint strength, intermetallic growth at the interface, and melting behavior of SAC305 solder alloy under multiple reflow cycles.

Materials and Methods

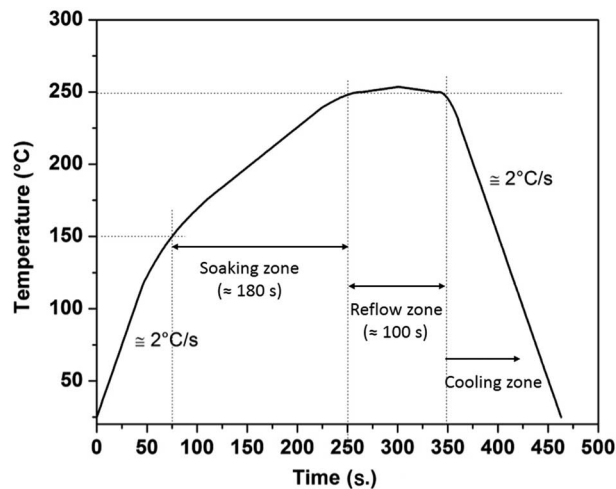
SPECIMEN PREPARATION AND JOINT SHEAR TEST

Commercial 96.5 tin-3 silver-0.5 copper (in wt.%) solder alloy paste (Persang Alloy Industries Pvt. Ltd. Gujarat, India) added with mildly activated rosin (ROLO) flux was used as the base alloy. The MWCNT with inner to outer diameter range of 10–25 nm and having an average length of 100–300 nm (Chengdu Organic Chemical Co. Ltd. Chinese Academy of Sciences, China) were used for reinforcement in the solder alloy. The scanning electron microscope (SEM) and transmission electron microscope (TEM) images with X-ray diffraction patterns for MWCNT used in this study are presented in [figure 1](#). Four solder systems were synthesized by mechanically dispersing MWCNT in 0.01, 0.05, 0.1, and 0.5 wt.% (related to the mass of solder paste), respectively, into the SAC305 solder paste. These solder systems are designated hereafter as SAC305- x MWCNT, where x represents the weight percentage addition of MWCNT. The required amount of MWCNT and solder paste were blended together for about 30 minutes to obtain the different compositions of the composite SAC305 solder alloy.

The joint shear strength of SAC305 composite solders was investigated through the tensile pull test of soldered lap joint specimens. The micro-lap-shear solder joint specimen used in this study is schematically represented in [figure 2](#). The specimen substrates were pure (99.9 % purity) electrical conductor grade copper plates with the surface roughness (R_a value) in the range of 0.1 to 0.3 μm . Copper plates were first precleaned with inorganic flux to remove the oxide layer followed by cleaning with acetone. A layer of solder paste that was 0.2 mm thick (0.1 gm) was sandwiched between the two copper plates. Specimens were assembled with the help of a fixture to maintain the rectangular shape of the solder joint with a 0.2-mm solder paste layer. The specimens were heated in an infrared integrated circuit heater reflow oven (Puhui T-962) using the thermal reflow profile represented in [figure 3](#). Specimens were subsequently subjected to 1, 2, 4, and 6 reflow cycles, respectively, to study the effect of multiple reflows on the solder joint properties. The shear test was performed using an Instron 5967 tensile testing machine (Instron, Norwood, MA) using the strain rate of $1 \times 10^{-2} \text{ s}^{-1}$ at the room

FIG. 3

Reflow temperature profile for copper/solder/copper joint preparation.



temperature. The average shear strength for the solder joint of each composite solder alloy was determined from the stress–strain curves obtained from the shear tests.

THERMAL ANALYSIS AND WETTABILITY TEST

The change in onset temperature, peak melting temperature, and melting range of SAC305 solder alloy with MWCNT addition was assessed using differential scanning calorimetry (DSC, 404 F1 Pegasus NETZSCH) under a nitrogen atmosphere. A composite solder specimen with a weight of 15.5 mg was placed in the aluminium crucible with a lid. A hole was made on the lid for the reaction outgas ventilation. The heating rate of 10°C/min for the temperature range of 30°C to 300°C was used for thermal analysis. The changes in the melting behavior of the composite solders were investigated by analyzing the heating curves obtained through the DSC test.

The change in wettability of the SAC305 solder alloy with different amounts of added MWCNT was determined with respect to the spreading area of composite solders. The measured amount (0.1 gm) of SAC305 solder paste (unreinforced and reinforced with different amounts of MWCNT) was placed on the polished copper cylindrical substrate using a solder paste dispenser. Specimens were reflowed in reflow oven by using thermal profile shown in [figure 3](#). The reflowed specimens were analyzed using a stereomicroscope (Stemi 2000-C, Zeiss, Oberkochen, Germany). The spreading area for all compositions was calculated using the image analyzer software (Axio Vision SE64 Rel. 4.9, Zeiss, Oberkochen, Germany).

MICROSTRUCTURE STUDY

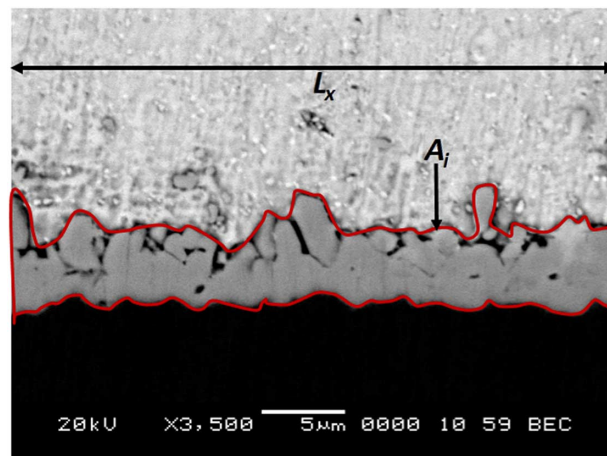
The development of solder joint microstructure and IMC growth at the joint interface with respect to MWCNT addition and multiple reflows were studied using scanning electron microscopy (SEM, JEOL JSM 6380LA, JEOL, Tokyo, Japan). Elemental analysis of different phases observed in the solder joint microstructure was carried out using energy dispersive spectroscopy (EDS). Reflowed specimens were cut and polished with the standard metallographic procedure. Polished surfaces were etched with 5 % nital solution (Ethanol [C₂H₅OH] and concentrated nitric acid in the 95+5 volume ratio, respectively) for 1–2 seconds. The interfacial IMC thickness was determined by image analysis using Axio Vision SE64 Rel. 4.9 software. IMC thickness was measured in three different regions at the interface for each specimen to obtain average thickness data. The IMC layer obtained at the interface was uneven in nature; hence, an average value of IMC thickness (\bar{x}) was determined by using equation (1).

$$\bar{x} = A_i / L_x \quad (1)$$

where A_i is the area and L_x is the length of IMC layer obtained from SEM micrograph represented in [figure 4](#).

FIG. 4

Representative SEM micrograph showing interfacial IMC layer of the solder joint after reflow.



Results and Discussion

THERMAL BEHAVIOR AND WETTABILITY

The effect of the addition of MWCNT in varying amounts on the melting behavior of SAC305 solder was investigated with the help of DSC heating curve analysis. Figure 5 shows DSC heating curves for monolithic and composite SAC305 solder specimens doped with different wt.% of MWCNT. The onset temperature, peak melting temperature, and melting range of SAC305 solder alloy with different compositions of MWCNT are presented in Table 1. The change in onset temperature (T_S) of SAC305 solder with the addition of MWCNT was negligible. The peak melting temperature (T_L) of composite solder alloy was observed to decrease slightly for minor additions (0.01–0.05 wt.%) of MWCNT, whereas additions above 0.05 wt.% increased the peak melting temperature by around 2°C. The decrease in the melting temperature of solder alloy with a low weight fraction of MWCNT reinforcement can be attributed to the increase in the surface instability because of the addition of surface active nanoparticles having high surface free energy. The excessive free energy contributed to the reduction in onset

FIG. 5 DSC curves for the heating cycle of SAC305 solder alloy with different wt.% of MWCNT: (A) SAC305, (B) SAC305-0.01MWCNT, (C) SAC305-0.05MWCNT, (D) SAC305-0.1MWCNT, and (E) SAC305-0.5MWCNT.

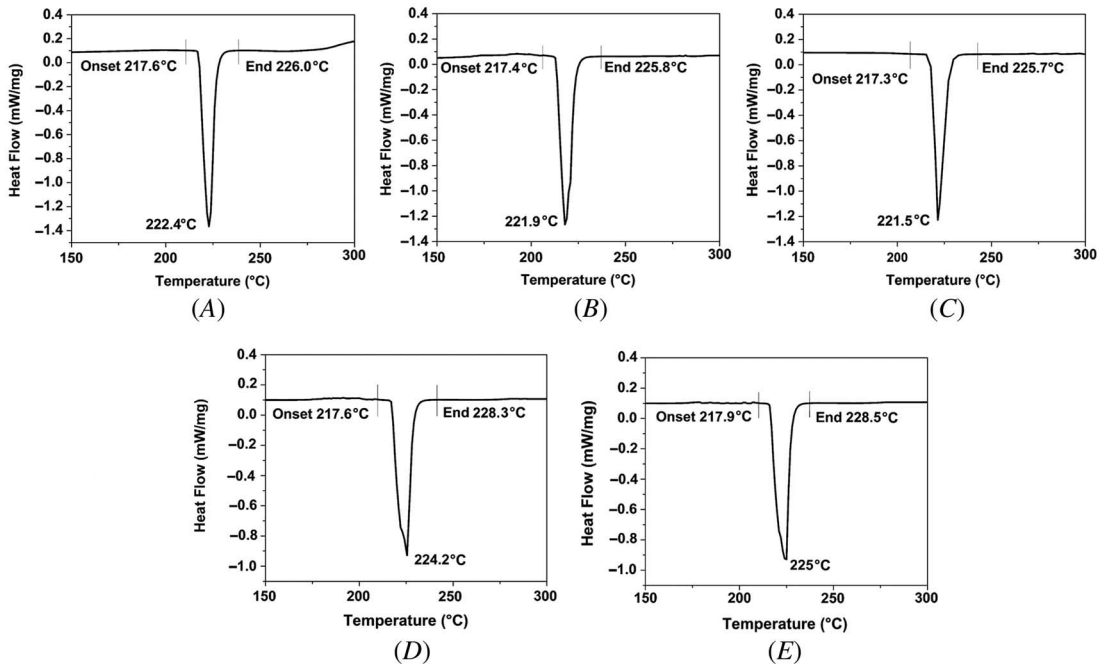


TABLE 1

Onset temperature, peak melting temperature, and melting range of SAC305 solder alloy with different MWCNT compositions

Solder Alloy Composition	Onset Temperature, T_S , °C	Peak Melting Temperature, T_L , °C	Melting Range, ΔT , °C
SAC305	217.6	222.4	4.8
SAC305-0.01MWCNT	217.4	221.9	4.5
SAC305-0.05MWCNT	217.3	221.5	4.2
SAC305-0.1MWCNT	217.6	224.2	6.6
SAC305-0.5MWCNT	217.9	225	7.1

FIG. 6

The spreading area as a function of the weight fraction of MWCNT addition.

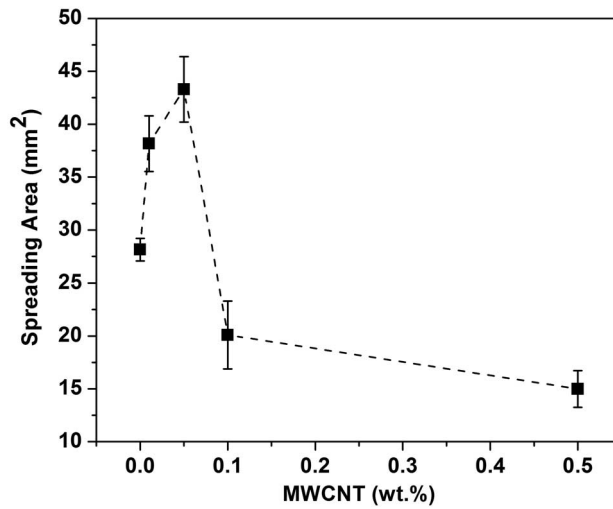
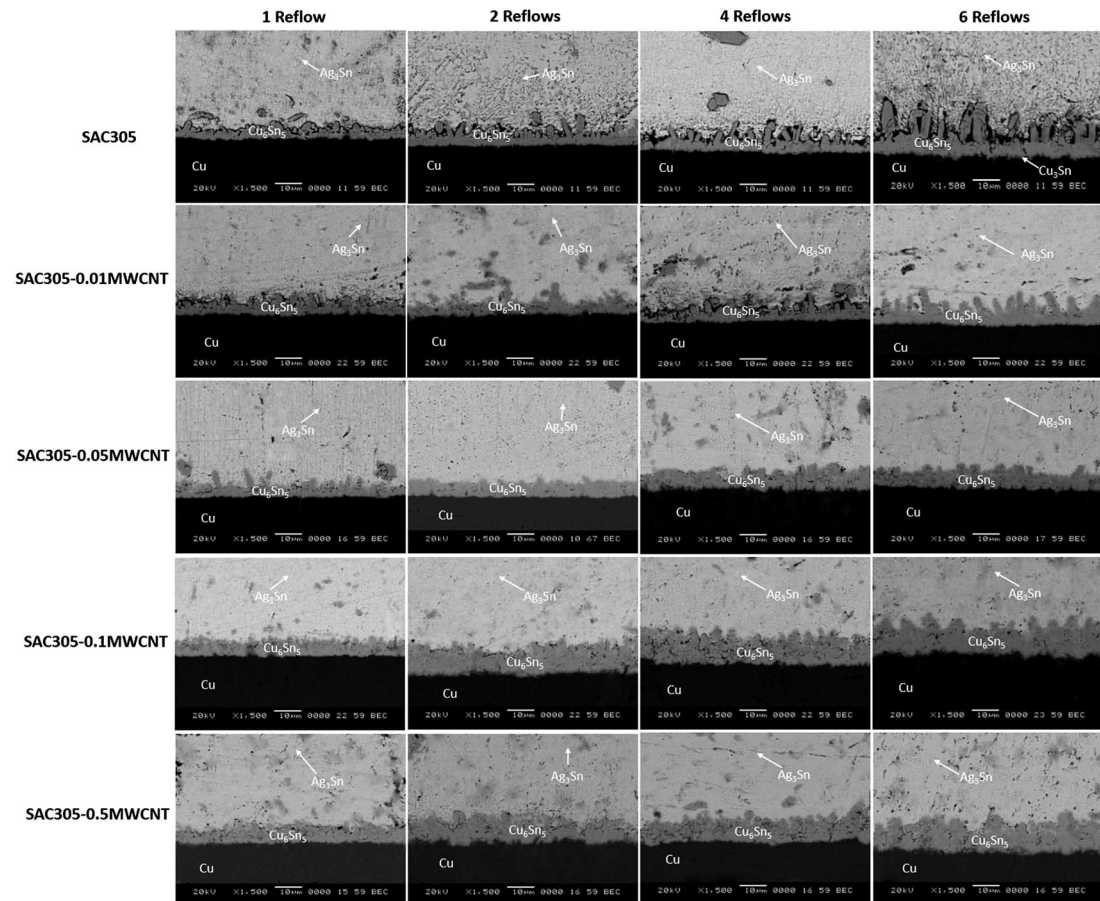


FIG. 7 SEM micrographs of the solder joint interface for monolithic and reinforced SAC305 with varying weight fractions of MWCNT for multiple reflow cycles.



as well as peak melting temperature of the composite solder. The addition of over 0.05 wt.% of MWCNT increases the agglomeration of nanoparticles into the solder, which reduces the effectiveness of nanoparticles and increases the melting point. The change in the melting range of SAC305 solder alloy with the compositions of 0.01–0.05 wt.% MWCNT was not significant, but the addition of 0.1–0.5 wt.% nanoparticles increased the melting range by about 1°C–2°C. The 0.05 wt.% MWCNT addition showed a noticeable drop in the peak melting temperature of solder alloy. The reduction in solder melting temperature improves the thermal reflow profile and indirectly decreases the thermal cost in electronics assembly production. The spreading area as a function of varying wt.% addition of MWCNT in SAC305 solder alloy is plotted in [figure 6](#). The addition of 0.01–0.05 wt.% MWCNT showed an increase in the spreading area, indicating an enhancement in the wettability of the SAC305 solder alloy. However, the spreading area decreased significantly after 0.1 wt.% MWCNT addition. The improvement in wettability of solder was prominent for 0.05 wt.% addition amongst all compositions tested. The addition of MWCNT in low-weight fractions enhanced the wettability of the solder by reducing the surface tension of liquid solder as well as decreasing the solder/substrate interfacial tension. The addition of nanoparticles beyond 0.05 wt.% increases the coagulation and network structure of MWCNT in the liquid solder, which increases the viscosity of the melt and blocks the melt flow, leading to a reduction in the spreading of the solder alloy.

SOLDER JOINT MICROSTRUCTURE

SEM micrographs of SAC305 solder/copper substrate joint interface for monolithic and composite solder alloy reflowed for multiple reflow cycles are presented in [figure 7](#). EDS analysis confirmed the presence of Cu_6Sn_5 IMC at the copper/solder interface and Ag_3Sn IMC in the solder matrix. EDS plots showing peaks for different IMC found in the microstructure with the percentage of the elemental composition are presented in [figure 8](#). The morphology and growth of Cu_6Sn_5 IMC changed with respect to the amount of MWCNT addition and reflow

FIG. 8 SEM images and EDS plots showing peaks for different IMC with the percentage of elemental composition: (A) Cu_6Sn_5 , (B) Cu_3Sn , and (C) Ag_3Sn .

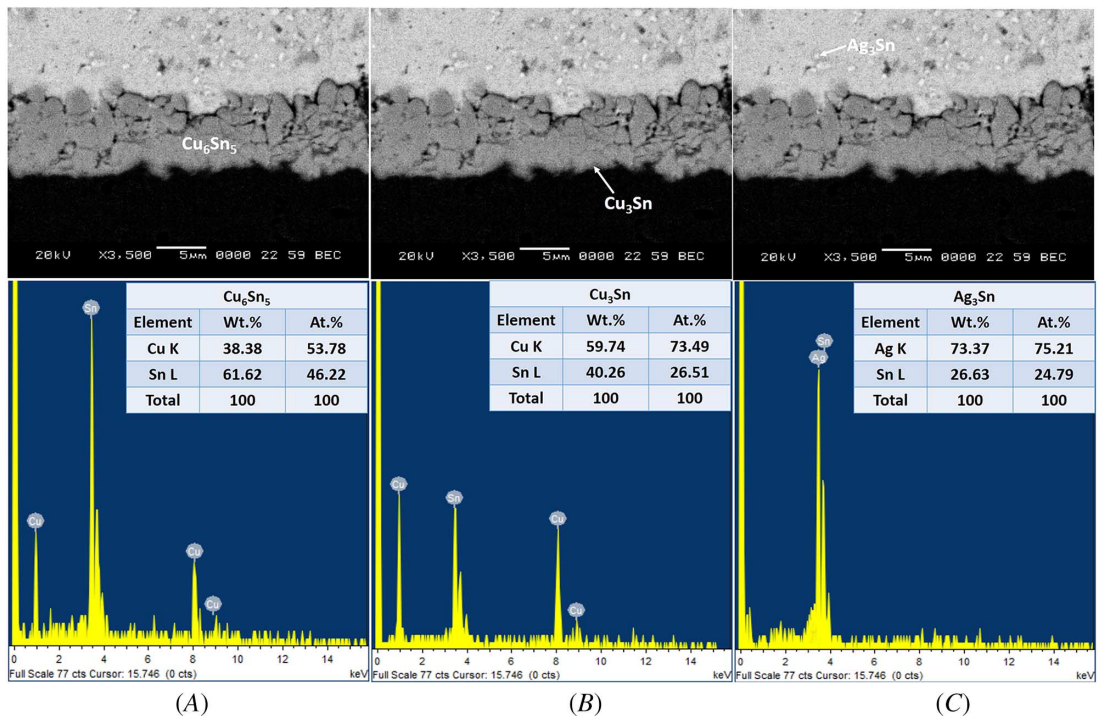
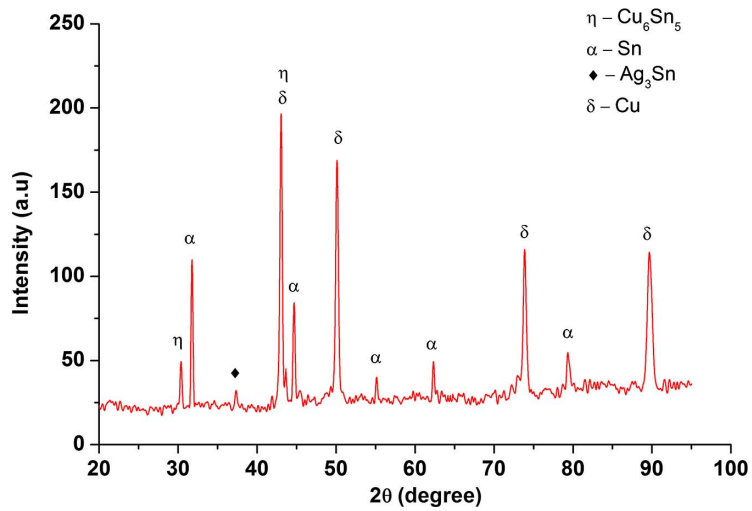
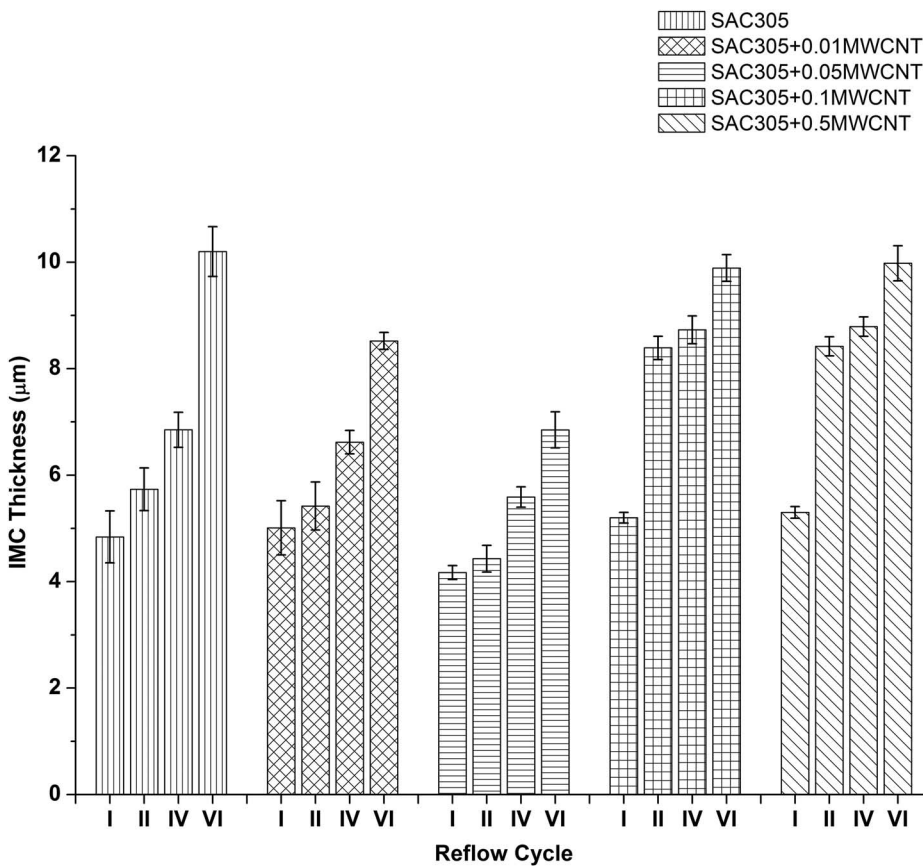


FIG. 9

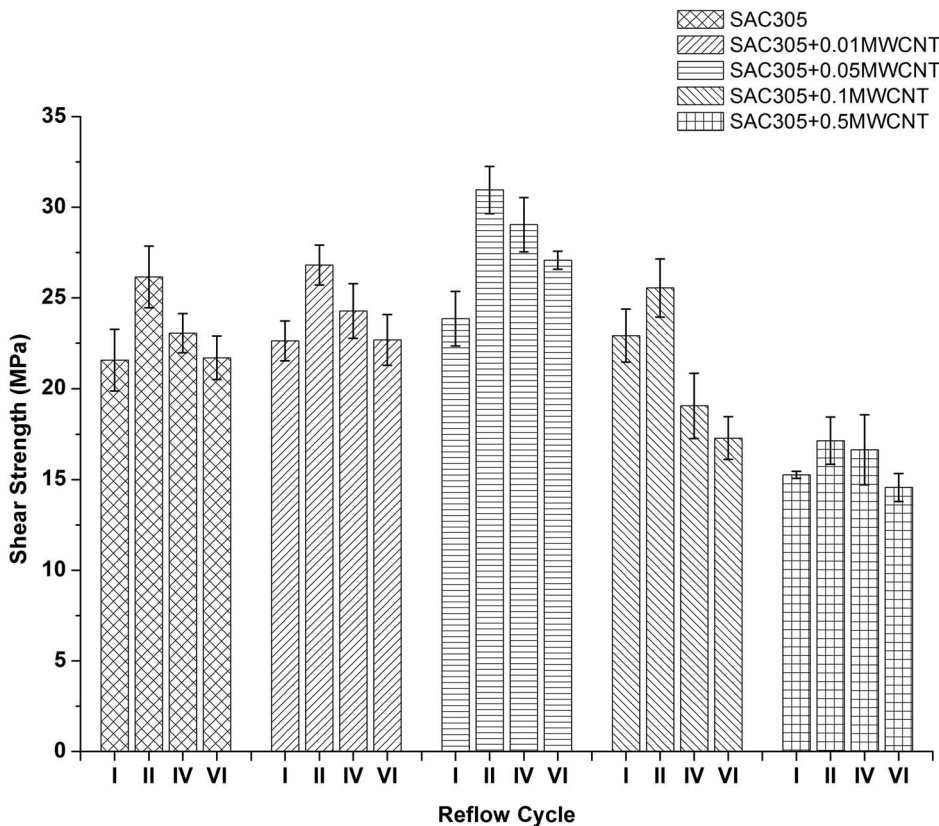
X-ray diffraction plot for SAC305 solder/copper substrate joint interface.

**FIG. 10** Average IMC thickness as a function of reflow cycle.

cycles. For unreinforced SAC305 solder, the morphology of Cu_6Sn_5 IMC appeared as scallop shaped and has grown elongated and thicker with higher reflow cycles. Microcracks were also observed in thick IMC layer for the specimens reflowed for six reflow cycles. The formation of thin and discontinuous Cu_3Sn IMC layer was observed between copper substrate and Cu_6Sn_5 IMC layer for the specimens reflowed for six reflow cycles. However, Cu_3Sn IMC was not observed for composite alloys under multiple reflow cycles. The addition of MWCNT in solder alloy changed the Cu_6Sn_5 IMC morphology to a rounded scallop shape. The IMC appeared more uniform under multiple reflow cycles. The Ag_3Sn IMC changed to a finer spheroidal morphology with increasing reflow cycles. The X-ray diffraction (XRD) plot taken at the interface represented in [figure 9](#) shows the peaks for all IMC present in the microstructure. The mean IMC thickness as a function of reflow cycle for SAC305 solder with different MWCNT compositions is shown in [figure 10](#).

The IMC thickness data revealed that the MWCNT addition in the range of 0.01–0.05 wt.% suppressed the Cu_6Sn_5 IMC growth under multiple reflow cycles. The compositions with 0.05 wt.% MWCNT addition being the most effective in IMC retardation. The Ag_3Sn IMC was observed in a finer spheroidal shape and was uniformly dispersed in tin matrix for all the compositions under multiple reflows. The optimum amount (0.05 wt.%) of MWCNT addition in SAC305 solder effectively fills the grain boundaries at the interface and inhibits the tin diffusion from the bulk solder to the interface, which suppresses the IMC growth under multiple reflow cycles. Excessive addition (0.1–0.5 wt.%) of MWCNT in solder increases the agglomeration and entanglement of MWCNT, leading to the loss of active surface energy and functionality of nanoparticles. The agglomeration reduces the net amount of dispersed active MWCNT in solder, which severely reduces the beneficial effects of MWCNT addition.

FIG. 11 Joint shear strength of SAC305 solder with different wt.% of MWCNT addition for 1, 2, 4, and 6 reflow cycles.



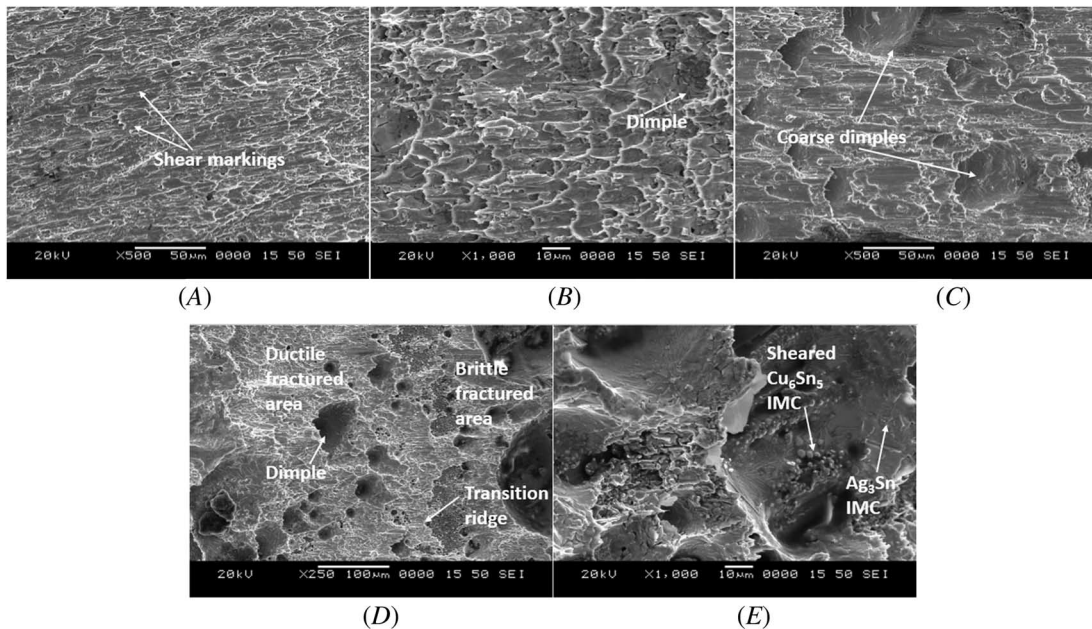
JOINT SHEAR STRENGTH

The shear strength of the SAC305 solder alloy with different compositions of MWCNT for 1, 2, 4, and 6 reflow cycles is shown in **figure 11**. The joint shear strength improved with the second reflow compared to first reflow cycle and decreased thereafter. The shear strength plot clearly indicates that the addition of 0.05 wt.% MWCNT improved the joint shear strength compared to unreinforced and other composites of the solder under multiple reflow cycles. Compared to unreinforced SAC305 solder alloy, SAC305-0.05MWCNT composition yielded about a 45 % increase in the joint shear strength after the second reflow. The thin and uniform Cu_6Sn_5 IMC layer formation at the interface and the uniform dispersion of fine spheroidal Ag_3Sn IMC in matrix contributed to enhancement in the joint shear strength. The uniformly dispersed fine spheroidal shaped Ag_3Sn IMC strengthened the matrix by a dispersion strengthening mechanism during shear failure. Additionally, the dispersed MWCNT in matrix helps in load transfer from matrix to nanotubes, which provides composite strength to the matrix under the applied stress condition. Dispersed Ag_3Sn IMC pins the grain boundaries and blocks the dislocation movement during shear, leading to an increase in the solder joint shear strength. The decrease in joint shear strength with higher reflow cycles is less prominent for SAC305-0.05 MWCNT composition compared to 0.1 and 0.5 weight fraction added compositions. The decrease in shear strength of the solder joint with the high weight fraction of MWCNT addition can be attributed to the decrease in solder wettability and thick Cu_6Sn_5 IMC at the interface. Thick and brittle IMC layers often possess microcracks that weaken the solder joint under the stress condition and reduce the joint shear strength.

FRACTOGRAPHY

The fractured surface analysis reveals the failure characteristics of sheared specimens. SEM images of fractured specimens after shear tests for SAC305 solder alloy with MWCNT addition are presented in **figure 12**. The fractured surface investigation revealed that the specimens for all the compositions mostly failed with mix-mode of failure. The unreinforced SAC305 solder alloy specimens reflowed up to four reflow cycles showed predominantly

FIG. 12 SEM images of fractured specimens after shear test for SAC305 solder alloy with MWCNT addition: (A) ductile fractured surface; (B) ductile fractured surface showing small dimples; (C) ductile fractured surface showing coarse dimples; (D) mixed mode fractured surface showing ductile and brittle fractured region along with transition ridge; (E) magnified dimple area showing broken Cu_6Sn_5 and Ag_3Sn IMC.



ductile fractured surface and small brittle failed area whereas, specimens after six reflow cycles failed with larger brittle area. The SEM image (fig. 12A) shows a typical ductile fractured surface of the sheared specimen for unreinforced SAC305 solder alloy. The specimens with the addition of 0.01–0.05 wt.% MWCNT exhibited ductile fracture with small dimples on the fractured surface under all the reflow conditions. Figure 12B shows the ductile failed region with small dimples on the surface. Specimens with SAC305-0.1 MWCNT composition failed with a ductile fracture having coarser dimples on the fractured surface (fig. 12C). The specimen for SAC305-0.5 MWCNT compositions showed the smaller ductile failed region with coarser dimples and larger brittle failed region separated by transition ridge. The magnified dimple region in figure 12E shows the shiny broken Cu_6Sn_5 IMC and Ag_3Sn IMC at the center of the coarse dimple in the micrograph. The fracture appeared to be propagating from bulk solder to the brittle Cu_6Sn_5 IMC layer at the interface. The transition of fracture mode from ductile to brittle was attributed to the thicker and coarser Cu_6Sn_5 IMC morphology at the interface.

Conclusion

The effect of the addition of MWCNT to SAC305 solder alloy on melting behavior, mechanical properties, microstructure evolution at the interface, and fracture behavior was investigated. The onset temperature (T_5) of SAC305 solder alloy with MWCNT reinforcement was not affected significantly. The peak melting temperature (T_L) and melting range of the SAC305 solder alloy decreased on addition of 0.01–0.05 wt.% MWCNT but increased with the addition in the range of 0.1–0.5 wt.%. The reinforcement in low-weight fractions (0.01–0.05 wt.%) of MWCNT improved the wettability, whereas excessive addition significantly decreased the wettability of SAC305 solder alloy. The SAC305-0.05 MWCNT composition showed significant retardation in IMC growth and consistent improvement in the joint shear strength of the solder joint under multiple reflow cycles. However, the addition of MWCNT above 0.05 wt.% significantly reduced the beneficial effect of the addition of nanoparticles.

References

1. L. C. Tsao, S. Y. Chang, C. I. Lee, W. H. Sun, and C. H. Huang, "Effects of Nano- Al_2O_3 Additions on Microstructure Development and Hardness of Sn3.5Ag0.5Cu Solder," *Materials & Design* 31, no. 10 (December 2010): 4831–4835, <https://doi.org/10.1016/j.matdes.2010.04.033>
2. T. Laurila, J. Hurtig, V. Vuorinen, and J. K. Kivilahti, "Effect of Ag, Fe, Au and Ni on the Growth Kinetics of Sn–Cu Intermetallic Compound Layers," *Microelectronics Reliability* 49, no. 3 (March 2009): 242–247, <https://doi.org/10.1016/j.microrel.2008.08.007>
3. A. S. M. A. Haseeb, Y. M. Leong, and M. M. Arafat, "In-Situ Alloying of Sn-3.5Ag Solder during Reflow through Zn Nanoparticle Addition and Its Effects on Interfacial Intermetallic Layers," *Intermetallics* 54 (November 2014): 86–94, <https://doi.org/10.1016/j.intermet.2014.05.011>
4. K. M. Kumar, V. Kripesh, and A. A. O. Tay, "Single-Wall Carbon Nanotube (SWCNT) Functionalized Sn–Ag–Cu Lead-Free Composite Solders," *Journal of Alloys and Compounds* 450, nos. 1–2 (February 2008): 229–237, <https://doi.org/10.1016/j.jallcom.2006.10.123>
5. J.-P. Salvetat-Delmotte and A. Rubio, "Mechanical Properties of Carbon Nanotubes: A Fiber Digest for Beginners," *Carbon* 40, no. 10 (August 2002): 1729–1734, [https://doi.org/10.1016/S0008-6223\(02\)00012-X](https://doi.org/10.1016/S0008-6223(02)00012-X)
6. S. M. L. Nai, J. Wei, and M. Gupta, "Effect of Carbon Nanotubes on the Shear Strength and Electrical Resistivity of a Lead-Free Solder," *Journal of Electronic Materials* 37, no. 4 (April 2008): 515–522, <https://doi.org/10.1007/s11664-008-0379-6>
7. S. M. L. Nai, J. Wei, and M. Gupta, "Influence of Ceramic Reinforcements on the Wettability and Mechanical Properties of Novel Lead-Free Solder Composites," *Thin Solid Films* 504, nos. 1–2 (May 2006): 401–404, <https://doi.org/10.1016/j.tsf.2005.09.057>
8. S. M. L. Nai, Y. D. Han, H. Y. Jing, C. M. Tan, J. Wei, and M. Gupta, "Using Nanoparticles and Carbon Nanotubes to Enhance the Properties of a Lead-Free Solder," *Nanotechnology 2009: Life Sciences, Medicine, Diagnostics, Bio Materials and Composites 2* (May 2009): 538–541.
9. S. Xu, X. Hu, Y. Yang, Z. Chen, and Y. C. Chan, "Effect of Carbon Nanotubes and Their Dispersion on Electroless Ni-P under Bump Metallization for Lead-Free Solder Interconnection," *Journal of Materials Science: Materials in Electronics* 25, no. 6 (June 2014): 2682–2691, <https://doi.org/10.1007/s10854-014-1929-8>
10. T. T. Dele-Afolabi, M. A. A. Hanim, M. Norkhairunnisa, H. M. Yusoff, and M. T. Suraya, "Growth Kinetics of Intermetallic Layer in Lead-Free Sn–5Sb Solder Reinforced with Multi-Walled Carbon Nanotubes," *Journal of Materials Science: Materials in Electronics* 26, no. 10 (October 2015): 8249–8259, <https://doi.org/10.1007/s10854-015-3488-z>

11. R. Mayappan, A. A. Hassan, N. A. A. Ghani, I. Yahya, and J. Andas, "Improvement in Intermetallic Thickness and Joint Strength in Carbon Nanotube Composite Sn-3.5Ag Lead-Free Solder," *Materials Today: Proceedings* 3, no. 6 (2016): 1338–1344, <https://doi.org/10.1016/j.matpr.2016.04.012>
12. C.-J. Lee, J. J. Moon, K.-H. Jung, and S.-B. Jung, "Thermal Characteristic of Sn-MWCNT Nanocomposite Solder in LED Package," in *IEEE 67th Electronic Components and Technology Conference* (Piscataway, NJ: Institute of Electrical and Electronics Engineers, 2017), 2225–2230, <https://doi.org/10.1109/ECTC.2017.167>
13. S. H. Kim, M.-S. Park, J.-P. Choi, and C. Aranas, "Improved Electrical and Thermo-Mechanical Properties of a MWCNT/In-Sn-Bi Composite Solder Reflowing on a Flexible PET Substrate," *Scientific Reports* 7, no. 1 (October 2017): 1–14, <https://doi.org/10.1038/s41598-017-14263-6>
14. L. Yang, H. Liu, and Y. Zhang, "Study on the Tensile Creep Behavior of Carbon Nanotubes-Reinforced Sn-58Bi Solder Joints," *Journal of Electronic Materials* 47, no. 1 (January 2018): 662–671, <https://doi.org/10.1007/s11664-017-5741-0>
15. H. Sun, Y. C. Chan, and F. Wu, "Reliability Performance of Tin–Bismuth–Silver (Sn57.6Bi0.4Ag) Solder Joints with Different Content of Carbon Nano-Tubes (CNTs) or Nickel (Ni)-Modified CNTs," *Journal of Materials Science: Materials in Electronics* 29, no. 10 (May 2018): 8584–8593, <https://doi.org/10.1007/s10854-018-8872-z>